HHS Public Access

Author manuscript

VipIMAGE 2019 (2019). Author manuscript; available in PMC 2020 July 22.

Published in final edited form as:

VipIMAGE 2019 (2019). 2019 October ; 34: 247–256. doi:10.1007/978-3-030-32040-9_26.

Toward an Affine Feature-Based Registration Method for Ground Glass Lung Nodule Tracking

Yehuda Kfir Ben Zikri[1], **María Helguera**[1], **Nathan D. Cahill**[2], **David Shrier**[3], **Cristian A. Linte**[4]

[1]Chester F. Carlson Center for Imaging Science, Rochester Institute of Technology, Rochester, NY, USA

[2]School of Mathematical Sciences, Rochester Institute of Technology, Rochester, NY, USA

[3]Division of Radiology, University of Rochester Medical Center, Rochester, NY, USA

[4]Biomedical Engineering and Chester F. Carlson Center for Imaging Science, Rochester Institute of Technology, Rochester, NY, USA

Abstract

Lung nodule progression assessment from medical imaging is a critical biomarker for assessing the course of the disease or the patient's response to therapy. CT images are routinely used to identify the location and size and rack the progression of lung nodules. However, nodule segmentation is challenging and prone to error, due to the irregular nodule boundaries, therefore introducing error in the lung nodule quantification process. Here, we describe the development and evaluation of a feature-based affine image registration framework that enables us to register two time point thoracic CT images as a means to account for the back-ground lung tissue deformation, then use digital subtraction images to assess tumor progression/regression. We have demonstrated this method on twelve de-identified patient datasets and showed that the proposed method yielded a better than 1.5mm registration accuracy vis-à-vis the widely accepted non-rigid image registration techniques. To demonstrate the potential clinical value of our described technique, we conducted a study in which our collaborating clinician was asked to provide an assessment of nodule progression/regression using the digital subtraction images post-registration. This assessment was consistent, yet provided more confidence, than the traditional lung nodule tracking based on visual analysis of the CT images.

Keywords

Lung nodule tracking; Affine feature-based image registration; Background tissue deformation correction; Quantitative nodule tracking

1 Introduction

Thin-slice helical chest CT images can help identify single pulmonary nodules [3] and classify them as either part-solid (also known as sub-solid) or solid nodules [2]. When

clinte@mail.rit.edu.

smaller than 1cm in diameter, these nodules are typically classified as incidental, benign findings that require follow-up CT [1]. Part-solid nodules feature a “ground-glass appearance”, hence commonly referred to as ground-glass opacities (GGO) nodules or ground-glass nodules (GGNs) and are characterized by hazy, increased opacities of the lung tissue that don’t completely obscure pulmonary structures. Moreover, pure GGNs feature only ground-glass appearance, with no solid component.

Longitudinal analysis and tracking of nodule progression in current clinical practice resorts to visual comparison between the initial and follow-up scans, as well as the use of diameter measurements, despite their frequent inaccuracy, to quantify growth rate. As such, the radiologist relies on manual one- (1D) or two-dimensional (2D) annotations to quantify the solid portion and the whole nodule size from the axial slices that show the largest lesion diameter and the visual appearance of the margins [6]. Subsequently, the lesion volume and volumetric growth rate such as the doubling time, may be estimated according to the shape approximation of the lesion depicted in the initial and the follow-up scans displayed side-by-side, with no prior registration of the initial and follow-up images.

Although three-dimensional (3D) assessment was suggested to provide more accurate and precise nodule measurements, especially for small nodules [6], volumetric analysis is rarely used in a typical clinical workflow, as it requires segmentation of the nodule. This process is time consuming and highly subjective to intra- and inter-observer variability, especially for GGNs with nodule margins that are often blurry and not easily distinctive. As such, volumetric assessment of nodule progression that relies on either manual or automated nodule segmentation is prone to ambiguity and may mislead diagnosis, hence rendering 2D slice-based analysis as the clinical standard of care for longitudinal lung nodule analysis.

Since GGNs are non-rigid structures that grow in an irregular fashion, their estimated 2D appearance and size may also be highly misleading. Not only is a single CT slice a poor predictor of the geometry, orientation, and volume of a 3D lesion, but the different appearance of the lesion between the initial and the follow-up scan may also be highly influenced by complex deformations of the surrounding tissues between the scans. Several factors may cause significant error in the nodule assessment: intrinsic factors, such as nodule orientation relative to the chest wall or other structures, irregular nodule margins, asymmetric nodule shape and attenuation; or extrinsic factors, including patient position, changes in the parenchyma surrounding the nodules, heart rate, and respiratory motion, which significantly changes lung volume and shape [6,13]. Zheng *et al.* [13] reported that estimates at end-inspiration vs. end-expiration may lead to nodule volume detection error on the order of 12% induced by local deformations alone. Similarly, an additional study [5] reported an overall ±18% mass (volume x HU) and volume measurement fluctuations of part-solid GGNs as a result of inter-scan variability, patient position, heart rhythm, and inspiration levels. These findings suggest that true, disease-induced nodule changes might be reliably detected only if a *significant* change in lesion size occurs [4], and must be separated from both the intrinsic and extrinsic nodule changes.

Current criteria for assessing lung ground glass nodule (GGN) growth rely on visual comparison and diameter measurements from axial slices of initial and follow-up CT images

that show the largest extent of the lesion, without any co-registration [6]. Volumetric analysis is rarely used clinically, as it requires segmentation of the nodule, which is highly inaccurate and could mislead diagnosis, since GGN boundaries are often blurry and not easily distinctive for segmentation. Moreover, the nodule appearance between the initial and follow-up scans is also influenced by complex deformations of the surrounding background lung tissue caused by changes in patient position, the parenchyma surrounding the nodules, heart rate, and respiratory motion, all of which significantly change lung volume and shape [13].

To objectively and accurately assess changes in GGN size and shape due to disease, the initial and follow-up CT images must first be co-registered, while accounting for any background lung tissue deformation that may influence the nodule size and geometry, not caused by the disease. To quantify the effect of extrinsic changes, such the background lung tissue deformation, on nodule geometry, and separate it from the disease-induced nodule changes, accurate registration of the initial and follow-up scans is a necessary precursor step [8,12]. Since the lung is a soft tissue organ, a rigid registration of the initial and follow-up scans will not capture the lung tissue deformation adequately.

Although deformable registration may be considered optimal, most deformable registration algorithms are highly dependent on the parameter initialization, are computationally inefficient, and pose a high risk of convergence to local rather than global minima, resulting in unrealistic deformations. As such, depending on the optimization trade-off between the similarity and regularization terms, if the registration is allowed to proceed extensively, the lesion depicted by the registered follow-up image will look similar to the lesion in the initial image, therefore compromising nodule progression assessment. As a result, the difficulty of assessing background lung tissue deformation and using it as a baseline when quantifying the disease-induced lesion changes still exists, and a reliable solution is still pending.

2 Methodology

To address this challenge, here we describe and validate a feature-based affine registration method to co-register the initial and follow-up lung CT images. This registration compensates for the back-ground lung deformation, such that the remaining differences in lesion size and shape attributable to the disease could be identified using a digitally subtracted image post-registration as suggested in [11].

2.1 Imaging Data

This study was conducted on ten pairs of chest CT datasets featuring an initial and follow-up scan. The CT image datasets were acquired on either a 16-slice Lightspeed or 64-slice VCT scanner (GE Medical Systems, Milwaukee, WI). All imaging data was retrieved following retrospective review of patient charts following informed consent granted by all patients, as approved by the Institutional Review Board. The ten datasets contained twelve lesions identified by two radiologists: one patient featured one lesion in each lung (Cases 5 and 6), while another patient featured two lesions in the same lung (Cases 11 and 12), with non-overlapping lesion ROIs. The datasets contained solitary GGNs, multiple GGNs, and solid nodules.

All scans were acquired in a single breath-hold with sub-millimeter resolution and featured lesions localized in different regions of the lung that showed different extent of progression as evaluated at different stages ranging from 0.5 months to almost 3 years. As an example, Case 9 featured a part-solid GGN with a large solid part attached to the chest wall, classified by both radiologists as a malignant juxtapleural nodule, justified by the large change detected at 32 month follow-up. Moreover, Case 2 featured a common transient part-solid nodule that showed almost complete regression in the follow-up scan. Lastly, Case 3 featured a new nodule in the follow-up scan that was not visible in the initial scan.

An expert radiologist manually segmented the nodules and also selected approximately 40 homologous fiducial landmarks on average, localized both within and in the vicinity of each lesion in both the initial and follow-up scans. Most landmarks were selected at vasculature branching points. According to the radiologists, these locations are least susceptible to non-rigid lung deformation due to breathing. The landmarks were used to quantify the TRE following each step of the registration pipeline.

2.2 Feature-Based Segmentation Overview

Following automatic segmentation and separation of the lungs from both the initial and follow-up CT scans, the registration was initialized by a centroid alignment of the lung- or lesion-centered region of interest (ROI), followed by a feature-based rigid registration. We used an approach that minimizes the chisquared statistic between the histograms of the initial and follow-up images to identify the optimal initial rotational transform. The subsequent feature-based registration method (Fig. 1) followed a modified formulation and implementation of the iterative closest point (ICP) algorithm.

The features used for registration were edges extracted from both the initial and follow-up CT scans using monogenic filtering [9]. Unlike the ICP algorithm in which the objective function minimizes the distance between estimated corresponding points using the closed-form solution of the Euclidean distance, we built a distance map [7] of the initial image by assigning each voxel a value equal to its distance from the closest edge.

We then multiplied the distance map of the initial edge image by the transformed follow-up edge image, then computed the sum of the distances from the transformed edges to the edges in the initial image, which served as the objective function to be minimized. Moreover, we separated the edges of the lung boundaries from the edges of the lung content and defined the Energy Dissimilarity (ED) function as the weighted sum of the distances between lung boundary edges and the lung content edges from the initial and follow-up scans. To identify the optimal weighting factor alpha, we evaluated the similarity metric (normalized cross-correlation (NCC)) for several values of alpha and selected the parameter value that yielded the highest NCC. The registration was implemented on both a lung-centered and a lesion-centered ROI.

2.3 Intensity-Based Deformable Registration

The result of the affine feature-based registration served as input for the last step of the registration pipeline—the deformable registration. Moreover, in the effort to quantify any potential shortcomings of the affine registration or improvements provided by an additional

deformable registration step, the intensity-based deformable registration also served as reference against which the affine feature-based registration was assessed. We used a high-degree of freedom diffeomorphic transformation method proposed in [10], with several pre-processing steps recommended by the authors, including the rescaling and truncation of the image intensities, followed by de-noising. This technique is referred to as the Greedy Symmetric Normalization (SyN) registration and is based on the LDDMM algorithm available via the ANTS (Advanced Normalization Tools) open source package integrated within ITK. This registration is initiated via a global affine registration on the lungs masks, rather than on the CT data. The mutual information (MI) similarity measure is used on four-level image pyramid together with gradient descent successive optimization. The successive optimization objective is controlling the affine registration parameters successively.

3 Results

We tested the developed registration algorithm on twelve image datasets consisting of initial and follow images of patients at various stage of disease. To assess registration accuracy, we computed the target registration error (TRE) across a set of 30–50 homologous fiducial markers selected by a collaborating radiologist in both the initial and follow-up scans.

We compared the TRE achieved using the proposed registration to the TRE achieved using the ANTS Symmetric Normalization deformable registration method deemed optimal by the EMPIRE10 lung registration challenge [10]. In addition, we used the residual fiducial registration error (FRE) across the homologous fiducial landmark datasets selected from the initial and follow-up images as a registration accuracy baseline control, as it assesses the homology of the landmarks based on a rigid least squared fit registration.

Our accuracy study showed differences on the order of 0.5mm between the TRE achieved using feature-based affine vs. deformable registration (Tables 1, 2 and Fig. 2), however with significant computing performance improvements (Tables 3 and 4) using the feature-based affine registration.

To visualize the registration results, we generated subtraction images i.e., initial (fixed) image minus the registered follow-up (moving) image from the lesion mid-slices after each registration. As mentioned earlier, subtraction images were shown to be efficient when assessing nodule growth-rate and reducing variability according to [11]. As shown in Fig. 3, both the affine and deformable registrations yielded similar visual results, with no significant visual differences.

4 Discussion and Conclusion

We described and validated a feature-based affine registration method designed to co-register initial and follow-up lung CT images to correct for the background lung tissue deformation to help objectively assess lung nodule changes induced by disease. Our study showed less than 1mm difference between the registration accuracy achieved using the feature-based affine registration, deformable registration, and baseline control registration, with significant performance improvement when using the affine registration. Moreover, the qualitative visual assessment conducted by two radiologists confirmed similar conclusions

about the nodule changes using the digital subtraction image post-registration as the current standard of care assessment method.

Acknowledgements

Research reported in this publication was supported by the National Institute of General Medical Sciences of the National Institutes of Health under Award No. R35GM128877 and by the Office of Advanced Cyber infrastructure of the National Science Foundation under Award No. 1808530.

References

1. Fischbach F, Knollmann F, Griesshaber V, Freund T, Akkol E, Felix R: Detection of pulmonary nodules by multislice computed tomography: improved detection rate with reduced slice thickness. Eur. Radiol 13, 2378–2383 (2003) [PubMed: 12743736]
2. Hansell DM, Bankier A, MacMahon H, McLoud TC, Müller NL, Remy J: Fleischner society: glossary of terms for thoracic imaging. Radiology 246(3), 697–722 (2008) [PubMed: 18195376]
3. Henschke CI, McCauley DI, Yankelevitz DF, Naidich DP, McGuinness G, Miettinen OS, Libby DM, Pasmantier MW, Koizumi J, Altorki NK, Smith JP: Early lung cancer action project: overall design and findings from baseline screening. Lancet 354, 99–105 (1999) [PubMed: 10408484]
4. Kakinuma R, Ashizawa K, Kuriyama K, Fukushima A, Ishikawa H, Kamiya H, Koizumi N, Maruyama Y, Minami K, Nitta N, Oda S, Oshiro Y, Kusumoto M, Murayama S, Murata K, Muramatsu Y, Moriyama N: Measurement of focal ground-glass opacity diameters on CT images. Interobserver agreement in regard to identifying increases in the size of ground-glass opacities. Acad. Radiol 19, 389–394 (2012) [PubMed: 22222027]
5. Kim H, Park CM, Lee SM, Lee HJ: Measurement variability of volume andmass in nodules with a solid portion less than or equal to 5 mm. Radiology 269, 585–593 (2013) [PubMed: 23864104]
6. Ko JP, Berman EJ, Kaur M, Babb JS, Bomsztyk E, Greenberg AK,Naidich DP, Rusinek H: Pulmonary nodules: growth rate assessment in patients by using serial CT and three-dimensional volumetry. Radiology 262, 662–671 (2012) [PubMed: 22156993]
7. Maurer CR, Qi R, Raghavan V: A linear time algorithm for computing exacteuclidean distance transforms of binary images in arbitrary dimensions. IEEE Transact. Pattern Anal. Mach. Intell 25(2), 265–270 (2003)
8. Oliveira FPM, Tavares JMRS: Medical image registration: a review. Comput.Methods Biomech. Biomed. Eng. Imaging Vis 17, 73–93 (2014)
9. Rajpoot K, Grau V, Noble JA: Local-phase based 3-D boundary detectionusing MONOGENIC signal and its application to real-time 3-D echocardiography images. In: Proceedings of IEEE International Symposium on Biomedical Imaging: From Nano to Macro 2009, pp. 783–786 (2009)
10. Song G, Tustison N, Avants B, Gee JC: Lung CT image registration usingdiffeomorphic transformation models. In: Medical Image Analysis for the Clinic: A Grand Challenge, pp. 23–32 (2010)
11. Staring M, Pluim JPW, de Hoop B, Klein S, van Ginneken B, Gietema H,Nossent G, Schaefer-Prokop C, van de Vorst S, Prokop M: Image subtraction facilitates assessment of volume and density change in ground-glass opacities in chest CT. Invest. Radiol 44, 61–66 (2009) [PubMed: 19104438]
12. Viergever MA, Maintz JB, Klein S, Murphy K, Staring M, Pluim JPW: A survey of medical image registration – under review. Med. Image Anal 33, 140–144 (2016) [PubMed: 27427472]
13. Zheng Y, Kambhamettu C, Bauer T, Steiner K: Accurate estimation of pulmonary nodule's growth rate in CT images with nonrigid registration and precise nodule detection and segmentation. In: 2009 IEEE Computer Society Conference on Computer Vision and Pattern Recognition Workshops, pp. 101–108. IEEE (2009)

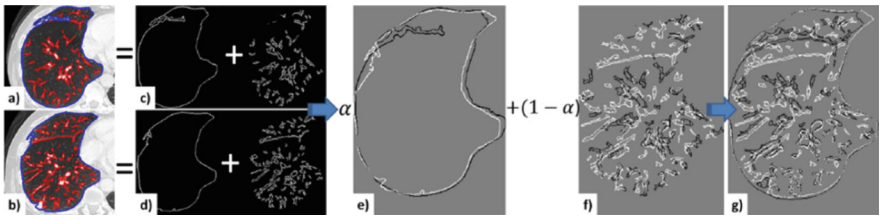

Fig.1.

Schematic of feature-based registration algorithm and computation of the similarity metric as a weighted sum between the distance map of the lung boundary and lung content.

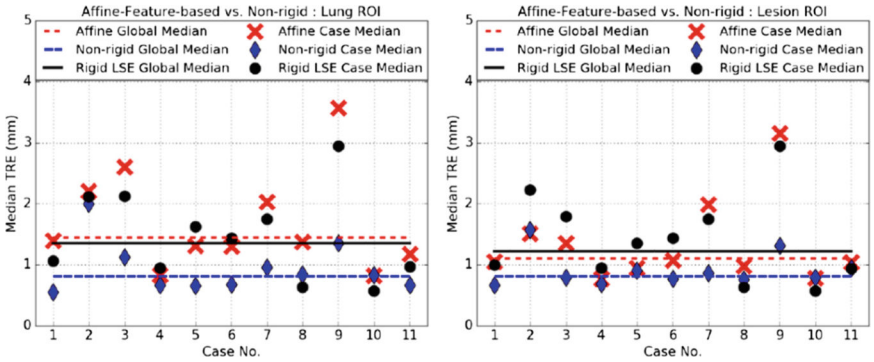

Fig.2.

Target registration error (TRE) comparison across 12 patient datasets between the feature-based affine registration, deformable registration, and baseline control (rigid least squared fit) registration for both the lung-centered ROI and lesion-centered ROI.

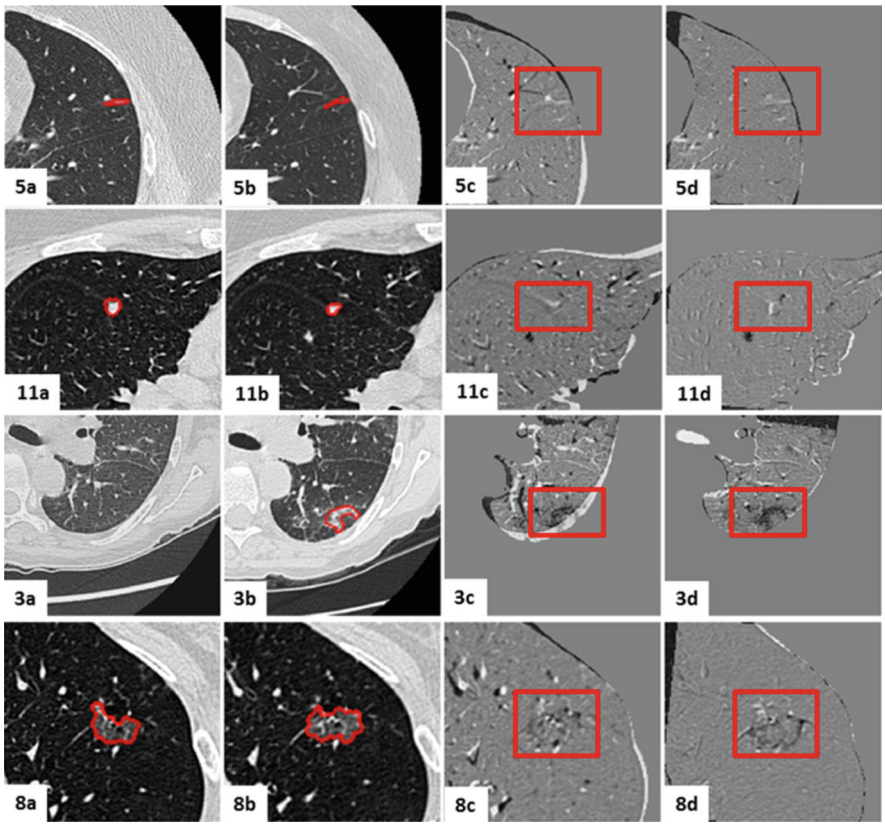

Fig.3.

Visual assessment of nodule changes: (a) initial image; (b) follow-up image; (c) digital subtraction image after centroid alignment; (d) digital subtraction image after feature-based affine registration. Four cases are showcased here: Case 5—no nodule change; Case 11—moderate nodule change; Case 3—new nodule appearing in follow-up image; and Case 8—severe nodule change.

Table 1.

Target registration error (TRE in mm) across 12 patient datasets for affine, deformable, and baseline registration performed on the lung-centered ROI.

Registration method	Mean ± Std. Dev. TRE (mm)	Median TRE (mm)
Affine registration	1.8 ± 1.6	1.4
Deformable registration	1.2 ± 1.2	0.8
Least square fit FRE (Control)	1.6 ± 1.1	1.3

Table 2.

Target registration error (TRE in mm) across 12 patient datasets for affine, deformable, and baseline registration performed on the lesion-centered ROI.

Registration method	Mean ± Std. Dev. TRE (mm)	Median TRE (mm)
Affine registration	1.5 ± 1.2	1.1
Deformable registration	1.2 ± 1.2	0.8
Least square fit FRE (Control)	1.5 ± 1.2	1.2

Table 3.

Performance (Mean ± Std. Dev. in minutes) comparison of affine and deformable intensity vs. feature-based registration performed on lung-centered ROI (357 × 248 × 455).

Registration method	Intensity-based registration (mins)	Feature-based registration (mins)
Affine registration	119.0 ± 10.3	8.0 ± 10.0
Deformable registration	245.0 ± 40.1	N/A

Table 4.

Performance (minutes) of rigid, affine, and deformable intensity- and feature-based registration performed on lesion-centered ROI.

Registration method	Intensity-based registration (mins)	Feature-based registration (mins)
Affine registration	1.3 ± 2.3	0.7 ± 1.5
Deformable registration	17.2 ± 10.2	N/A